

**Bayesian analysis of inflationary features in Planck and SDSS data**Micol Benetti<sup>\*</sup> and Jailson S. Alcaniz<sup>†</sup>*Observatório Nacional, 20921-400 Rio de Janeiro, Rio de Janeiro, Brazil*

(Received 27 April 2016; published 28 July 2016)

We perform a Bayesian analysis to study possible features in the primordial inflationary power spectrum of scalar perturbations. In particular, we analyze the possibility of detecting the imprint of these primordial features in the anisotropy temperature power spectrum of the cosmic microwave background (CMB) and also in the matter power spectrum  $P(k)$ . We use the most recent CMB data provided by the Planck Collaboration and  $P(k)$  measurements from the 11th data release of the Sloan Digital Sky Survey. We focus our analysis on a class of potentials whose features are localized at different intervals of angular scales, corresponding to multipoles in the ranges  $10 < \ell < 60$  (Oscill-1) and  $150 < \ell < 300$  (Oscill-2). Our results show that one of the step potentials (Oscill-1) provides a better fit to the CMB data than does the featureless  $\Lambda$ CDM scenario, with *moderate* Bayesian evidence in favor of the former. Adding the  $P(k)$  data to the analysis weakens the evidence of the Oscill-1 potential relative to the standard model and strengthens the evidence of this latter scenario with respect to the Oscill-2 model.

DOI: 10.1103/PhysRevD.94.023526

**I. INTRODUCTION**

The inflationary paradigm offers an elegant theoretical framework in which the emergence of the primordial curvature perturbations can be understood. In the simplest inflationary scenarios a primordial scalar perturbation with a nearly scale-invariant power spectrum is generated by a single minimally coupled scalar field  $\phi$  rolling down a smooth potential  $V(\phi)$ . This framework seems to agree with the most recent cosmic microwave background (CMB) data [1,2], which show a preference for plateau-like<sup>1</sup> over monomial potentials, as well as no compelling statistical evidence for a specific class of scenarios (we refer the reader to [7–11] for different points of view of the current observational status of inflation).

Recently, several works have analyzed inflationary models that account for localized features in the primordial power spectrum, showing in some cases a better fit to the data with respect to a smooth power-law spectrum [12–22]. Features in the primordial power spectrum can be generated following departures from the slow-roll approximation, which can happen in more general inflationary scenarios with a symmetry-breaking phase transition. Examples are the inflationary models with a step in the primordial potential, whose oscillation in the power spectrum of curvature perturbations is localized around the scale that crosses the horizon at the time the phase transition occurs [23,24].

In principle, this oscillation could be seen in several observables, such as in the CMB maps and in the

large-scale galaxy distribution, since the primordial scalar fluctuation is the seed for all the cosmic structures currently observed. It is therefore expected that data of the temperature anisotropy power spectrum as well as measurements of the matter power spectrum  $P(k)$  from galaxy surveys may provide hints on the origin of these features. Originally, steplike inflationary potentials were postulated to study the “glitch” appearing at the low- $\ell$  region of the CMB anisotropy spectrum. The signatures of this class of models in the CMB temperature power spectrum and bispectrum [17–21,25–31] and in the tensor spectrum [32,33] have been studied in detail using the current data and have shown a consistent improvement of the  $\Delta\chi^2$  values with respect to the featureless  $\Lambda$ CDM model.

In this work we proceed a step further in this kind of analysis and employ a Bayesian statistical analysis to verify the predictions of a class of inflationary steplike potential models and discuss their observational viability in a wide range of scales, considering their observational consequences not only on the present CMB anisotropy temperature maps but also on the matter power spectrum  $P(k)$ . We work with two data sets: the second CMB data release of the Planck Collaboration [2,34] and a combination of these CMB data with measurements of the matter power spectrum from the Baryon Oscillation Spectroscopic Survey (BOSS) CMASS Data Release-11 sample of the Sloan Digital Sky Survey (DR11-SDSS) experiment (hereafter “CMB + SDSS”) [35]. We perform a Bayesian analysis using both the Metropolis-Hastings algorithm implemented in COSMOMC [36] and the nested sampling algorithm of MULTINEST [37–39]. We find that at least one of the scenarios studied is able to provide a better fit to the CMB and CMB +  $P(k)$  data than does the standard  $\Lambda$ CDM model.

<sup>\*</sup>micolbenetti@on.br<sup>†</sup>alcaniz@on.br<sup>1</sup>For plateau-like potentials  $V(\phi) \rightarrow 0$  as  $\phi \rightarrow \infty$  (see, e.g., [3–6]).

This paper is organized as follows. Section II reviews the class of inflationary models considered in this work. We also discuss observational data sets and priors used in the analysis as well as the Bayesian model selection method adopted. In Sec. III we discuss the results and present a brief comparison with previous analysis. We end the paper by summarizing the main results in Sec. IV.

## II. MODEL AND METHOD

Relaxing the slow-roll condition leaves traces on the primordial power spectrum. For example, if the wavelengths cross the horizon during the fast-roll phase, one must expect deviations from the usual power-law power spectrum. The brief violation of the slow-roll condition can be shaped, in a single-field model, by adding a local feature, such as a step, to an otherwise flat potential. Following the formalism presented in Refs. [23,40,41], we consider a model with a local feature added to a chaotic potential

$$V(\phi) = \frac{1}{2}m^2\phi^2 \left[ 1 + c \tanh\left(\frac{\phi - b}{d}\right) \right]. \quad (1)$$

The spectrum of primordial perturbations, resulting from the potential (1), is found to be essentially a power law with superimposed oscillations. These are centered on a value that depends on the parameter  $b$ , with amplitude set by  $c$  and damping given by  $d$ . Asymptotically, the spectrum recovers the familiar  $k^{n_s-1}$  form, typical of slow-roll inflationary models.

In this work we adopt an analytical parametrization for the scalar primordial spectrum resulting from Eq. (1), as studied in [25],

$$P_R(k) = \exp \left[ \ln P_0(k) + \frac{A_f}{3} \frac{k\eta_f}{\sinh(\frac{k\eta_f}{x_d})} W'(k\eta_f) \right], \quad (2)$$

where

$$W'(x) = \left( -3 + \frac{9}{x^2} \right) \cos 2x + \left( 15 - \frac{9}{x^2} \right) \frac{\sin 2x}{2x}, \quad (3)$$

$P_0(k) = A_s \left(\frac{k}{k_*}\right)^{n_s-1}$  is the smooth spectrum with the standard power-law form,  $A_f$  is the kinetic energy perturbation of the step,  $\eta_f$  is the step crossing time in units of Mpc, and  $x_d$  is the dimensionless damping scale. The oscillating window function  $W'(k\eta_f)$  is modulated by the decaying envelope  $k\eta_f / \sinh(k\eta_f/x_d)$  which is set by the details of the step. It is worth mentioning that the approximate approach of Eqs. (2) and (3) allows one to significantly save computing time with respect to the full numerical solution of the evolution equations for the potential of Eq. (1), without a meaningful loss of accuracy [20].

We consider a “vanilla” model with the addition of features in the primordial spectrum, parametrized as in

Eqs. (2) and (3). In our analysis, we vary the usual cosmological parameters, namely, the physical baryon density,  $\Omega_b h^2$ , the physical cold dark matter density,  $\Omega_c h^2$ , the ratio between the sound horizon and the angular diameter distance at decoupling,  $\theta$ , the optical depth,  $\tau$ , the primordial scalar amplitude,  $\mathcal{A}_s$ , the primordial spectral index,  $n_s$ , and the additional  $A_f$ ,  $\eta_f$ , and  $x_d$  step parameters. We also vary the nuisance foreground parameters [34] and consider purely adiabatic initial conditions. The sum of neutrino masses is fixed to 0.06 eV, and we limit the analysis to scalar perturbations with  $k_0 = 0.05 \text{ Mpc}^{-1}$ .

The posterior probabilities distributions of the parameters are generated using both the Metropolis-Hastings algorithm implemented in COSMOMC [36] and the nested sampling algorithm of MULTINEST [37–39]. We use a modified version of the CAMB [42] code in order to compute the CMB anisotropies spectrum for different values of the parameters describing the steplike inflationary model, as in Eqs. (2) and (3). The Gelman and Rubin criteria [43,44] are used to evaluate the convergence of the Monte Carlo Markov chain (MCMC) analysis, demanding that  $R - 1 \leq 0.02$ . In our Bayesian analysis we use the most accurate importance nested sampling (INS) [39,45] instead of the vanilla nested sampling (NS), requiring INS global log-evidence error  $< 0.1$ .

### A. Priors

As mentioned earlier, the class of models considered in this analysis is able to produce localized oscillations in the primordial power-law potential. The oscillation spot is set by the parameter  $\eta_f$  in Eqs. (2) and (3) and depends on the scale where the wavelengths cross the horizon. We note that, for increasing values of the step crossing time parameter, the oscillation is shifted to larger scales (lower multipoles), until it disappears completely from the temperature angular power spectrum of the CMB (TT spectrum) for values of  $\ln(\eta/\text{Mpc}) > 10$ . At the same time, for values of  $\ln(\eta/\text{Mpc}) < 5$  the oscillation is shifted to the high- $\ell$  part of the spectrum, i.e., to scales without interest to the present study.

Previous works [20,46] identified two different ranges of multipoles for these oscillations from the data: the first one lies in the interval  $10 < \ell < 60$  (hereafter Oscill-1), whereas the second one lies in the interval  $150 < \ell < 300$  (hereafter Oscill-2). In particular, these oscillation ranges are distinguished by different priors on the  $A_f$  parameter, i.e.,  $A_f > 0.5$  for Oscill-1 and  $A_f < 0.5$  for Oscill-2. We run our preliminary test following the guidelines of the previous studies, i.e., assuming the same priors on the feature parameter  $A_f$ , and setting for the parameters  $\ln(\eta_f/\text{Mpc})$  and  $\ln x_d$  the intervals [5:10] and [−1:5], respectively. Using the COSMOMC we found the value where the step parameter posterior probability drops to zero, and we set the priors for our analysis as shown in Table I. In order to estimate the impact of the prior choice

TABLE I. Priors on the feature parameters of Eqs. (2) and (3).

Parameter	Prior (Oscill-1)	Prior (Oscill-2)
$A_f$	Uniform(0.5, 1)	Uniform(0, 0.2)
$\ln \eta_f$	Uniform(7, 8)	Uniform(6.5, 8)
$\ln x_d$	Uniform(0, 1)	Uniform(3, 5)

on the  $A_f$  parameter, we also repeat the analysis using the relaxed priors  $A_f[0:1]$ ,  $\ln(\eta_f/\text{Mpc})[5.5:8.5]$ ,  $\ln x_d[0:2]$ .

It is important to highlight the central role played, in the COSMOMC analysis, by the prior ranges choice, since the introduced  $\eta_f$  and  $x_d$  step parameters show multimodal posterior probability distributions. The MCMC analysis, indeed, can fail to fully explore all peaks which contain significant probability, especially if the peaks are very narrow. The MULTINEST algorithm, on the contrary, does not show the same analysis problem. For this reason we use the COSMOMC code only for the preliminary parameters estimation, and we present in this work only the MULTINEST analysis results.

### B. Data sets

We use the second release of Planck data [2,34] (hereafter TT + lowP), namely the high- $\ell$  Planck temperature data (in the range of  $30 < \ell < 2508$ ) from the 100, 143, and 217 GHz half-mission TT cross spectra and the low-P data by the joint TT, EE, BB, and TE likelihood (in the range of  $2 < \ell < 29$ ). More precisely, the latter data come from the best-fit temperature map obtained by the commander component separation algorithm applied to Planck 30–857 GHz data, jointly with the Wilkinson Microwave Anisotropy Probe (WMAP) 9-year observations between 23 and 94 GHz [47] and the Haslam *et al.* 408 MHz survey [48]; the E and B maps are obtained from the 70 GHz maps using their 30 and 353 GHz maps as foreground templates.

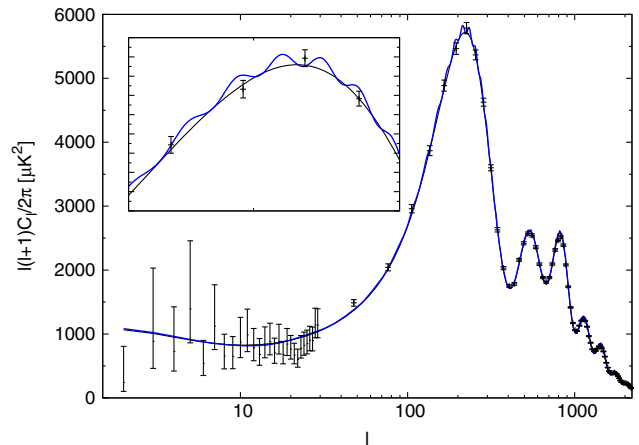
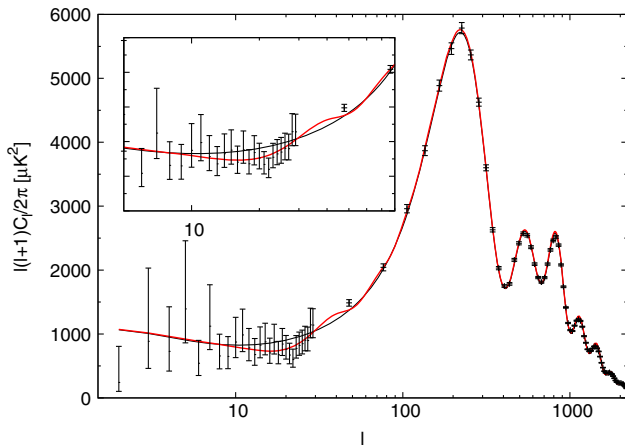


FIG. 1. Temperature power spectrum for the two inflationary steplike models best-fit values in comparison with the  $\Lambda$ CDM model best fit (black line). Left: best-fit values for the Oscill-1 model using TT + lowP data. The inset is a zoom at  $5 < \ell < 80$ . Right: best-fit values for the Oscill-2 model using CMB + SDSS data. The inset is a zoom at  $150 < \ell < 280$ .

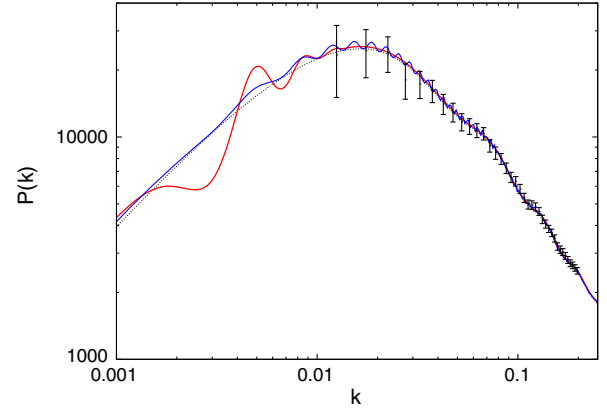


FIG. 2. Matter power spectrum for the best-fit  $\Lambda$ CDM model (dotted black line) and for the two steplike models: Oscill-1 best-fit values using TT + lowP data (red line), Oscill-2 best-fit values using CMB + SDSS data (blue line).

We combine the CMB data with the matter power spectrum measurements from the BOSS CMASS Data Release-11 sample (covering the redshift range  $z = 0.43\text{--}0.7$ ) of the DR11-SDSS experiment (CMB + SDSS). We use the data sets of [35] and publicly available in the SDSS Collaboration website (<http://www.sdss3.org>).

The best-fit CMB angular spectra and the matter power spectra for Oscill-1 and Oscill-2 models are shown in Figs. 1 and 2. In order to obtain the results we use binned high- $\ell$  TT data for the analysis of the Oscill-1 model since this type of oscillation is placed in the low- $\ell$  region of the spectrum, which means that details on the high- $\ell$  part do not add any information. On the other hand, for the Oscill-2 model the oscillations are located at small scales and show higher frequency (see Fig. 1, right panel). Therefore, for the analysis of this latter model we use the unbinned version of the high- $\ell$  TT data in order to maximize the sensitivity of sharp features that lie inside the single bin.

### C. Statistical model selection

In order to probe possible features in the primordial inflationary power spectrum, we perform a Bayesian model comparison considering three models, namely, the standard  $\Lambda$ CDM scenario and the two models with localized oscillations in the power-law potential named earlier as Oscill-1 and Oscill-2. In this kind of analysis the “best” model is the one that achieves the best compromise between quality of fit and predictivity. Indeed, while a model with more free parameters will always fit the data better (or at least as good as) a model with fewer parameters, such added complexity ought to be avoided whenever a simpler model provides an adequate description of the observations. The Bayesian model comparison offers a formal way to evaluate whether the extra complexity of a model is required by the data, preferring the model that describes the data well over a large fraction of their prior volume. In this section, we briefly review the model comparison and introduce our notation (we refer the reader to [49–52] for some recent applications of Bayesian model selection in cosmology).

Let us consider two competing models,  $M_i$  and  $M_j$ , whose  $n_j$  parameters (of model  $M_j$ ) are common to  $M_i$ , which in turn has  $n_i - n_j$  extra parameters. The posterior probability for the parameters vector  $\theta$  (of length  $n_i$ ) given the data  $x$  under the model  $M_i$  comes from Bayes’ theorem,

$$p(\theta|x, M_i) = \frac{p(x|\theta, M_i)\pi(\theta|M_i)}{p(x|M_i)}, \quad (4)$$

and similarly for  $M_j$ . The term  $p(x|\theta, M_i)$  is the likelihood, while  $\pi(\theta|M_i)$  is the prior probability distribution function. The normalization constant in the denominator is called *evidence*  $\mathcal{E}$ , and it is the marginal likelihood for the model  $M_i$ ,

$$p(x|M_i) \equiv \mathcal{E}_{M_i} = \int d\theta p(x|\theta, M_i)\pi(\theta|M_i). \quad (5)$$

The posterior probability of the  $M_i$  model given the data are written as

$$p(M_i|x) \propto \mathcal{E}_{M_i}\pi(M_i). \quad (6)$$

Assuming no *a priori* preference about any model [ $\pi(M_j) = \pi(M_i)$ ], the ratio of the posterior probabilities of the two models (the so-called *Bayes factor*) is given by

$$\mathcal{B}_{ij} = \frac{\mathcal{E}_{M_i}}{\mathcal{E}_{M_j}}. \quad (7)$$

The more complex model  $M_i$  will (if  $M_j$  is nested) inevitably lead to a higher (or at least equal) likelihood, but the evidence will favor the simplest model if the fit is nearly as good, through the smaller prior volume. We

TABLE II. Confidence limits of 68% for the cosmological and step parameters. The second and third columns refer to a minimal  $\Lambda$ CDM model with a featureless spectrum, using binned high- $\ell$  TT data; the fourth and fifth columns show the constraint of the inflationary steplike model using Oscill-1 prior of Table I and binned high- $\ell$  TT data; the sixth and seventh columns show the constraint of the inflationary steplike model using Oscill-2 prior of Table I and unbinned high- $\ell$  TT data. The  $\Delta\chi^2_{\text{best}}$  and the  $\ln\mathcal{B}_{MM'}$  of Oscill-2 analysis refer to the difference with respect to the  $\Lambda$ CDM analysis using the unbinned high- $\ell$  TT data. These results refer to the Bayesian analysis results of the MULTINEST code analysis.

Parameter	$\Lambda$ CDM model		Oscillation-1		Oscillation-2	
	TT+lowP	CMB+SDSS	TT+lowP	CMB+SDSS	TT+lowP	CMB+SDSS
$100\Omega_b h^2$	$2.225 \pm 0.02$	$2.232 \pm 0.02$	$2.222 \pm 0.021$	$2.229 \pm 0.02$	$2.225 \pm 0.021$	$2.233 \pm 0.02$
$\Omega_c h^2$	$0.1194 \pm 0.0019$	$0.1182 \pm 0.0017$	$0.1202 \pm 0.0019$	$0.1188 \pm 0.0017$	$0.1195 \pm 0.0019$	$0.1183 \pm 0.0017$
$100\theta$	$1.04091 \pm 0.00043$	$1.04104 \pm 0.00042$	$1.04108 \pm 0.00045$	$1.04097 \pm 0.00042$	$1.04094 \pm 0.00043$	$1.04111 \pm 0.00040$
$\tau$	$0.083 \pm 0.008$	$0.084 \pm 0.008$	$0.083 \pm 0.008$	$0.084 \pm 0.008$	$0.083 \pm 0.008$	$0.083 \pm 0.008$
$n_s$	$0.9664 \pm 0.0052$	$0.9685 \pm 0.0050$	$0.9637 \pm 0.0052$	$0.9660 \pm 0.0050$	$0.9667 \pm 0.0053$	$0.9685 \pm 0.0049$
$\ln 10^{10} A_s^a$	$3.100 \pm 0.0162$	$3.099 \pm 0.0166$	$3.102 \pm 0.0164$	$3.100 \pm 0.0166$	$3.100 \pm 0.0163$	$3.097 \pm 0.0170$
$A_f$	...	...	$0.75 \pm 0.14$	$0.75 \pm 0.13$	$0.037 \pm 0.027$	$0.04 \pm 0.02$
$\ln \eta_f/\text{Mpc}$	...	...	$7.18 \pm 0.10$	$7.18 \pm 0.09$	$7.316 \pm 0.39$	$7.21 \pm 0.33$
$\ln x_d$	...	...	$0.49 \pm 0.27$	$0.49 \pm 0.27$	$3.92 \pm 0.57$	$4.0 \pm 0.5$
$\sigma_8$	$0.835 \pm 0.009$	$0.829 \pm 0.009$	$0.836 \pm 0.009$	$0.831 \pm 0.009$	$0.834 \pm 0.009$	$0.828 \pm 0.009$
$H_0^b$	$67.48 \pm 0.83$	$68.00 \pm 0.74$	$67.10 \pm 0.85$	$67.72 \pm 0.73$	$67.42 \pm 0.85$	$67.98 \pm 0.73$
$\Delta\chi^2_{\text{best}}$	...	...	5.8	5	1.7	8.4
$\ln\mathcal{B}_{ij}^c$	...	...	$3.91 \pm 0.03$	$1.82 \pm 0.03$	$0.58 \pm 0.04$	$-1.64 \pm 0.07$

<sup>a</sup> $k_0 = 0.05 \text{ Mpc}^{-1}$ .

<sup>b</sup>[ $\text{kms}^{-1} \text{Mpc}^{-1}$ ].

<sup>c</sup>The associated error is calculated with the simple error propagation formula, assuming that the two measurements are uncorrelated:  $\sigma^2(\ln\mathcal{B}_{ij}) = \sigma^2(\ln\mathcal{E}_i) + \sigma^2(\ln\mathcal{E}_j)$ .

assume uniform (and hence separable) priors in each parameter, such that  $\pi(\theta|M_i) = (\Delta\theta_1 \cdots \Delta\theta_{n_i})^{-1}$  and

$$\mathcal{B}_{ij} = \frac{\int d\theta p(x|\theta, M_i) (\Delta\theta_1 \cdots \Delta\theta_{n_i})}{\int d\theta' p(x|\theta', M_j) (\Delta\theta'_1 \cdots \Delta\theta'_{n_i})}. \quad (8)$$

In order to rank the models of interest, we adopted the following scale to interpret the values of  $\ln \mathcal{B}_{ij}$  in terms of the strength of the evidence of a chosen reference model ( $M_j$ ):  $\ln \mathcal{B}_{ij} = 0-1$ ,  $\ln \mathcal{B}_{ij} = 1-2.5$ ,  $\ln \mathcal{B}_{ij} = 2.5-5$ , and  $\ln \mathcal{B}_{ij} > 5$  indicate, respectively, an *inconclusive*, *weak*, *moderate*, and *strong* preference of the model  $M_i$  with respect to the model  $M_j$ . Note that negative values of  $\ln \mathcal{B}_{ij}$  means support in favor of the model  $M_j$ . We refer to [50] for a more complete discussion about this scale that is a revised and more conservative version of the so-called *Jeffreys' scale* [53].

### III. RESULTS

The main quantitative results of our analysis are shown in Table II. First, we assume the minimal  $\Lambda$ CDM model and use the CMB and CMB + SDSS data sets discussed earlier. From Fig. 3 one can see that the addition of the galaxy data (solid line) shows a preference for lower values of  $\Omega_c h^2$  and for higher values of  $n_s$ , with respect to the analysis using only CMB (TT + lowP) data. From Table II we also note a slight improvement of the constraints on the Hubble parameter  $H_0$  and a preference for a higher value of  $\sigma_8$ . A good concordance between the results using binned and unbinned high- $\ell$  TT data is verified. For brevity, however, we report in Table II only the  $\Lambda$ CDM analysis using the binned high- $\ell$  TT data. It is also worth mentioning that the values of  $\Delta\chi^2_{\text{best}}$  and  $\ln \mathcal{B}_{ij}$  for the Oscill-2 model are obtained with respect to the  $\Lambda$ CDM analysis using the unbinned high- $\ell$  TT data.

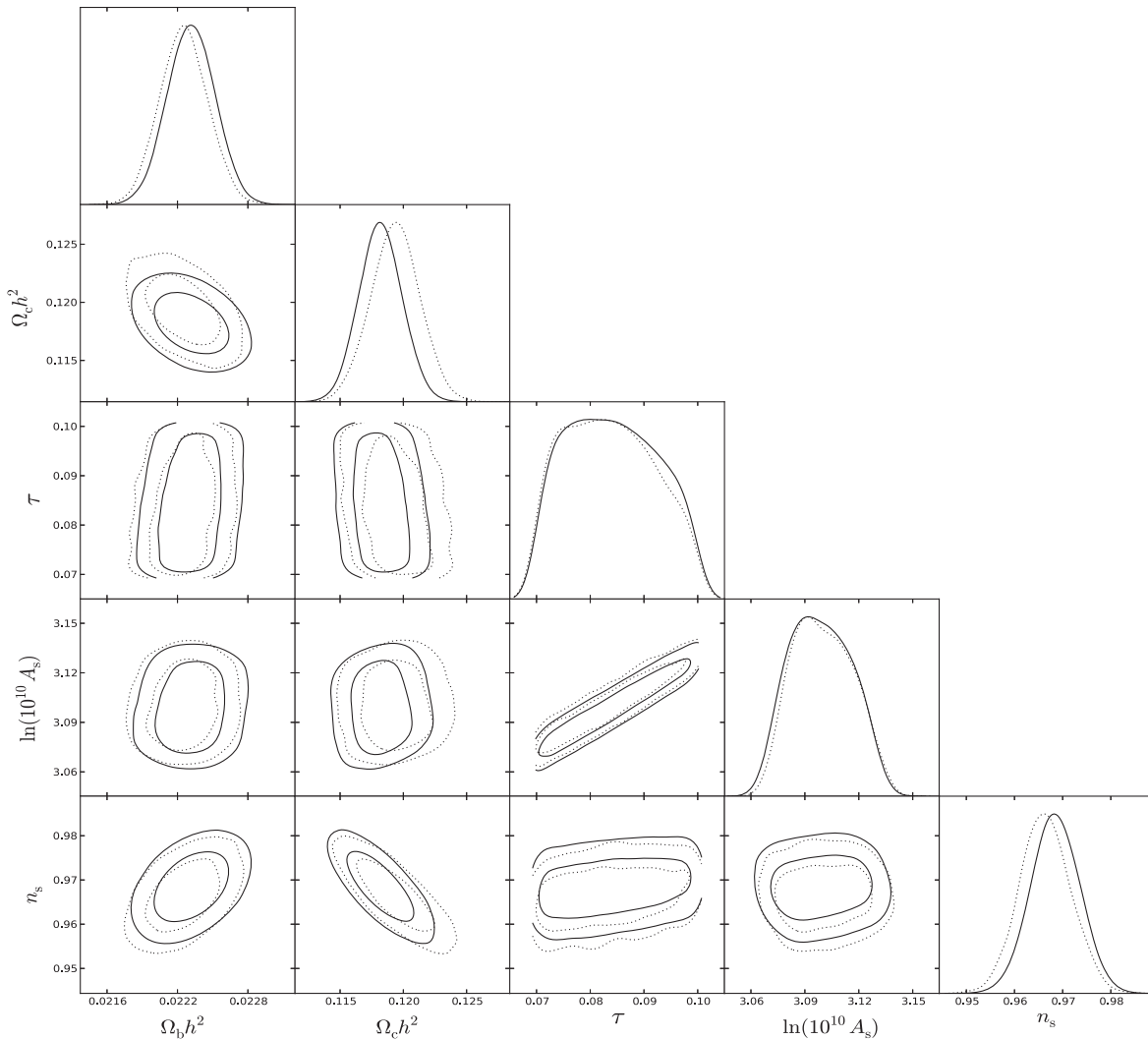


FIG. 3. Confidence regions of 68% and 95% on the  $\Lambda$ CDM model for Planck TT + lowP data (black dotted line) and CMB + SDSS data (black solid line). The numerical results of these analyses are reported in the second and third columns Table II.

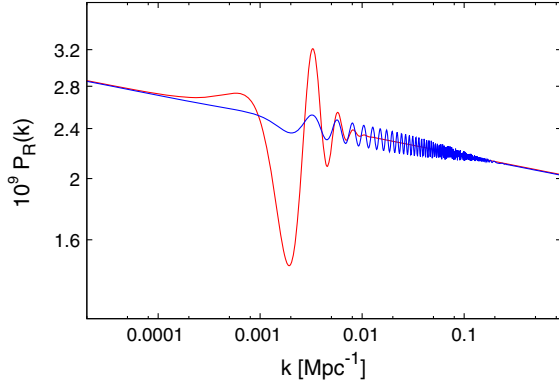


FIG. 4. Primordial power spectrum for the two step models: Oscill-1 (red line) with  $A_f = 0.75$ ,  $\ln(\eta/\text{Mpc}) = 7.18$  and  $\ln x_d = 0.49$  and Oscill-2 (blue line) with  $A_f = 0.04$ ,  $\ln(\eta/\text{Mpc}) = 7.21$ , and  $\ln x_d = 4$ .

For the central mean values given in Table II, we show in Fig. 4 the primordial scalar power spectrum for the two step models. We note that the two primordial oscillations start around the same scale (approximately the same value of  $\eta_f$ ) but show very different amplitude and damping properties, which in turn produce very different features. The primordial power spectrum of the Oscill-1 model (red line) has a high amplitude and damping parameter values, and produces features at the scale interval  $10^{-3} \lesssim k \lesssim 10^{-2}$ . In principle, this makes it possible to detect them using only CMB data, since the current LSS data cover scales of  $k \gtrsim 10^{-2}$  [35].

In Fig. 5 we show the posterior probability distribution for the step parameter values. As expected, the addition of the large-scale structure data improves the constraints on these parameters, mainly those related to the Oscill-2 model whose features extend to lower scales (see Fig. 4). In comparison with the TT + lowP constraints (blue dashed line), we note the tighter constraints on the frequency parameter  $\ln \eta_f/\text{Mpc}$ , which for the CMB + SDSS data show a bimodal distribution.

Table II also shows that the constraints on the usual cosmological model parameters are not significantly affected by the presence of primordial features. Moreover, in the case of the Oscill-1 model, our bounds on the step parameters are consistent with previous analysis [20] using the first Planck release (2013) with the only exception of the amplitude parameter  $A_f$ , which now prefers lower values. On the other hand, our results for the TT + lowP data also show *moderate* evidence ( $\ln \mathcal{B}_{ij} = 3.91 \pm 0.03$ ) in favor of the Oscill-1 model with respect to the  $\Lambda\text{CDM}$  scenario. If we relax the step parameter priors to

$$A_f[0:1], \quad \ln(\eta_f/\text{Mpc})[5.5:8.5], \quad \ln x_d[0:2], \quad (9)$$

the *moderate* evidence of Oscill-1 becomes *weak*, and the distribution of probability shows a weak secondary peak, which extends the explored parameter space. Our results seem to be in disagreement with those of the Planck Collaboration [2], where a featureless primordial potential is preferable over the steplike models. Actually, the

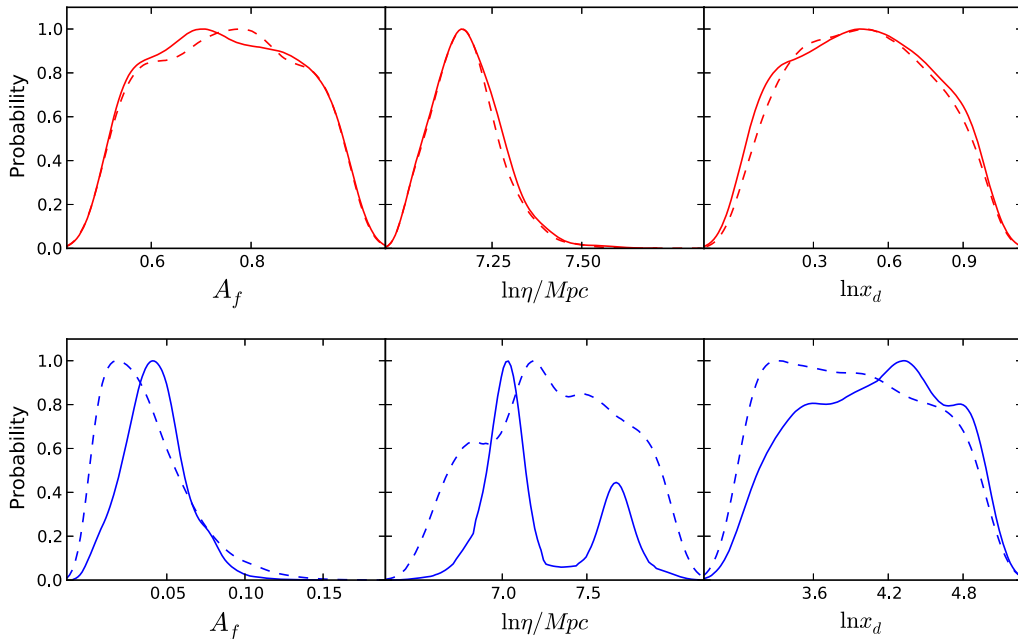


FIG. 5. One-dimensional posterior probability densities. Top: Oscill-1 step parameters analysis reported in Table II fourth and fifth columns, using TT + lowP data (red dashed line) and CMB + SDSS data (red solid line). Bottom: Oscill-2 step parameters analysis reported in the sixth and seventh columns of Table II using TT + lowP data (blue dashed line) and CMB + SDSS data (blue line).

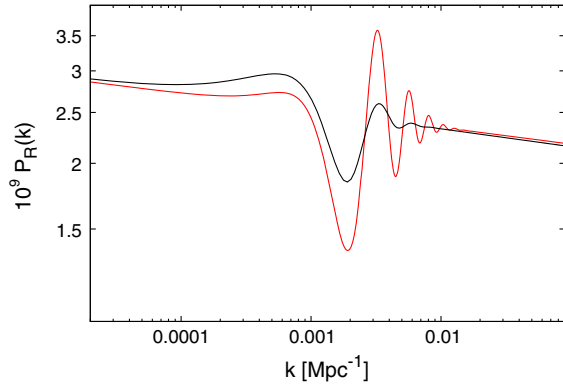


FIG. 6. Primordial power spectrum for the Oscill-1 best-fit model (red line) with  $A_f = 0.728$ ,  $\ln(\eta/\text{Mpc}) = 7.20$  and  $\ln x_d = 0.75$ , and for the parametrization discussed in the Planck-2015 analysis [2] (black line) with the best-fit values  $A_f = 0.347$ ,  $\ln(\eta/\text{Mpc}) = -3.10$ , and  $\ln x_d = 0.342$ .

constrained oscillation in Ref. [2] refers to a different parametrization model [21] and shows different step parameter values, whose overall effect is to produce smaller and deeper oscillations with respect to the results of this work, as shown in Fig. 6. At the same time, the parametrization used in this work produced a different behavior in the scales immediately before where the oscillation occurs.

For the Oscill-2 model, our analysis shows *inconclusive* evidence ( $\ln \mathcal{B}_{ij} = 0.58 \pm 0.04$ ) relative to the  $\Lambda$ CDM scenario using the TT + lowP data set. We also observe that the addition of  $P(k)$  data weakens the evidence of the Oscill-1 model relative to the standard cosmology and strengthens the evidence of this latter with respect to the Oscill-2 model.

#### IV. CONCLUSION

We have performed a Bayesian model selection statistics to compare the observational viability of a class of inflationary models with steplike features in the inflaton potential and the  $\Lambda$ CDM cosmology using the most up-to-date CMB and LSS data sets. The steplike inflationary potentials studied are able to produce features in the primordial scalar power spectra, inducing an oscillation in the anisotropy power spectrum with magnitude, extent, and position which depend on three step parameters. We have considered two types of models beyond the minimal  $\Lambda$ CDM model: the Oscill-1 model, whose features lie in the multipole range  $10 < \ell < 60$ , and the Oscill-2 model, which produces features at multiples  $150 < \ell < 300$  (see Fig. 1).

In order to perform our analysis, we have used an approximate form of the power spectrum, as given in Eqs. (2) and (3), and two data sets: the most recent data release of the Planck Collaboration (TT + lowP) and this CMB data set added to the  $P(k)$  measurements from the DR11 of the SDSS Collaboration. For the  $\Lambda$ CDM model, our analysis shows a good concordance between the results using the CMB data only and the extended data set (CMB + SDSS). As the main result of this analysis, we have shown that the Oscill-1 model provides a better fit to current CMB data than does the standard  $\Lambda$ CDM model, with *moderate* Bayesian evidence in favor of the steplike potential (Oscill-1). Such a result, however, seems to be in disagreement with the one reported by the Planck Collaboration, in which a featureless primordial potential is preferable over the steplike models. When the extended data set (CMB + SDSS) is considered, the evidence of the Oscill-1 model relative to the standard cosmology becomes *weak*, just as the Bayesian evidence of the  $\Lambda$ CDM cosmology with respect to the Oscill-2 model.

Finally, as shown in Fig. 1, our best-fit scenario (the Oscill-1 model) deviates significantly from the standard model only at very low values of  $k$ . We, therefore, expect to verify the reality of these features in the CMB and matter power spectra with data from the future release of the Planck Collaboration, as well as from the next generation of very deep galaxy surveys like, for example, the Dark Energy Spectroscopic Instrument [54] and the Javalambre Physics of the Accelerating Universe Astrophysical Survey [55].

#### ACKNOWLEDGMENTS

M. B. acknowledges financial support from the Fundação Carlos Chagas Filho de Amparo à Pesquisa do Estado do Rio de Janeiro (FAPERJ) through the post-doc *Nota 10* fellowship. J. S. A. is supported by Conselho Nacional de Desenvolvimento Científico e Tecnológico (CNPq), Instituto Nacional de Ciência e Tecnologia de Estudos do Espaço (INEspaço), and FAPERJ. The authors thank Sérgio Fontes, Antonio França, and Eduardo Matera for their assistance and acknowledge the use of COSMOMC [42] and the MULTINEST codes [37–39]. We are also grateful to Florian Beutler for helpful discussions and to the anonymous referee for the good comments and recommendations.

- [1] P. A. R. Ade *et al.* (Planck Collaboration), [arXiv:1502.01589](#).
- [2] P. A. R. Ade *et al.* (Planck Collaboration), [arXiv:1502.02114](#).
- [3] A. A. Starobinsky, *Phys. Lett.* **91B**, 99 (1980).
- [4] E. D. Stewart, *Phys. Rev. D* **51**, 6847 (1995).
- [5] G. R. Dvali and S. H. H. Tye, *Phys. Lett. B* **450**, 72 (1999).
- [6] J. P. Conlon and F. Quevedo, *J. High Energy Phys.* **01** (2006) 146.
- [7] J. Martin, [arXiv:1502.05733](#).
- [8] A. Ijjas, P. J. Steinhardt, and A. Loeb, *Phys. Lett. B* **723**, 261 (2013).
- [9] A. Linde, [arXiv:1402.0526](#).
- [10] A. H. Guth, D. I. Kaiser, and Y. Nomura, *Phys. Lett. B* **733**, 112 (2014).
- [11] R. H. Brandenberger, *Classical Quantum Gravity* **32**, 234002 (2015).
- [12] H. V. Peiris *et al.* (WMAP Collaboration), *Astrophys. J. Suppl. Ser.* **148**, 213 (2003).
- [13] L. Covi, J. Hamann, A. Melchiorri, A. Slosar, and I. Sorbera, *Phys. Rev. D* **74**, 083509 (2006).
- [14] J. Hamann, L. Covi, A. Melchiorri, and A. Slosar, *Phys. Rev. D* **76**, 023503 (2007).
- [15] M. J. Mortonson, C. Dvorkin, H. V. Peiris, and W. Hu, *Phys. Rev. D* **79**, 103519 (2009).
- [16] D. K. Hazra, M. Aich, R. K. Jain, L. Sriramkumar, and T. Souradeep, *J. Cosmol. Astropart. Phys.* **10** (2010) 008.
- [17] P. D. Meerburg, R. Wijers, and J. P. van der Schaar, *Mon. Not. R. Astron. Soc.* **421**, 369 (2012).
- [18] M. Benetti, M. Lattanzi, E. Calabrese, and A. Melchiorri, *Phys. Rev. D* **84**, 063509 (2011).
- [19] M. Benetti, S. Pandolfi, M. Lattanzi, M. Martinelli, and A. Melchiorri, *Phys. Rev. D* **87**, 023519 (2013).
- [20] M. Benetti, *Phys. Rev. D* **88**, 087302 (2013).
- [21] V. Miranda and W. Hu, *Phys. Rev. D* **89**, 083529 (2014).
- [22] B. Hu and J. Torrado, *Phys. Rev. D* **91**, 064039 (2015).
- [23] J. A. Adams, B. Cresswell, and R. Easther, *Phys. Rev. D* **64**, 123514 (2001).
- [24] P. Hunt and S. Sarkar, *Phys. Rev. D* **70**, 103518 (2004).
- [25] P. Adshead, C. Dvorkin, W. Hu, and E. A. Lim, *Phys. Rev. D* **85**, 023531 (2012).
- [26] P. Adshead, W. Hu, C. Dvorkin, and H. V. Peiris, *Phys. Rev. D* **84**, 043519 (2011).
- [27] N. Bartolo, D. Cannone, and S. Matarrese, *J. Cosmol. Astropart. Phys.* **10** (2013) 038.
- [28] A. G. Cadavid, A. E. Romano, and S. Gariazzo, *Eur. Phys. J. C* **76**, 385 (2016).
- [29] S. Mooij, G. A. Palma, G. Panotopoulos, and A. Soto, *J. Cosmol. Astropart. Phys.* **10** (2015) 062; **02** (2016) E01.
- [30] J. R. Fergusson, H. F. Gruetjen, E. P. S. Shellard, and M. Liguori, *Phys. Rev. D* **91**, 023502 (2015).
- [31] J. R. Fergusson, H. F. Gruetjen, E. P. S. Shellard, and B. Wallisch, *Phys. Rev. D* **91**, 123506 (2015).
- [32] V. Miranda, W. Hu, and C. Dvorkin, *Phys. Rev. D* **91**, 063514 (2015).
- [33] V. Miranda, W. Hu, and P. Adshead, *Phys. Rev. D* **89**, 101302 (2014).
- [34] N. Aghanim *et al.* (Planck Collaboration), [arXiv:1507.02704](#).
- [35] F. Beutler *et al.* (BOSS Collaboration), *Mon. Not. R. Astron. Soc.* **443**, 1065 (2014).
- [36] A. Lewis and S. Bridle, *Phys. Rev. D* **66**, 103511 (2002).
- [37] F. Feroz, M. P. Hobson, and M. Bridges, *Mon. Not. R. Astron. Soc.* **398**, 1601 (2009).
- [38] F. Feroz and M. P. Hobson, *Mon. Not. R. Astron. Soc.* **384**, 449 (2008).
- [39] F. Feroz, M. P. Hobson, E. Cameron, and A. N. Pettitt, [arXiv:1306.2144](#).
- [40] J. A. Adams, G. G. Ross, and S. Sarkar, *Phys. Lett. B* **391**, 271 (1997).
- [41] J. A. Adams, G. G. Ross, and S. Sarkar, *Nucl. Phys.* **B503**, 405 (1997).
- [42] A. Lewis, A. Challinor, and A. Lasenby, *Astrophys. J.* **538**, 473 (2000).
- [43] A. Gelman and D. B. Rubin, *Stat. Sci.* **7**, 457 (1992).
- [44] S. Brooks and A. Gelman, *J. Comput. Graph. Stat.* **7**, 434 (1998).
- [45] E. Cameron and A. Pettitt, *Stat. Sci.* **29**, 397 (2014).
- [46] P. A. R. Ade *et al.* (Planck Collaboration), *Astron. Astrophys.* **571**, A22 (2014).
- [47] C. L. Bennett *et al.* (WMAP Collaboration), *Astrophys. J. Suppl. Ser.* **208**, 20 (2013).
- [48] C. G. T. Haslam, C. J. Salter, H. Stoffel, and W. E. Wilson, *Astron. Astrophys. Suppl. Ser.* **47**, 1 (1982).
- [49] A. R. Liddle, *Mon. Not. R. Astron. Soc.* **377**, L74 (2007).
- [50] R. Trotta, *Mon. Not. R. Astron. Soc.* **378**, 72 (2007).
- [51] D. Parkinson, P. Mukherjee, and A. R. Liddle, *Phys. Rev. D* **73**, 123523 (2006).
- [52] B. Santos, N. C. Devi, and J. S. Alcaniz, [arXiv:1603.06563](#).
- [53] H. Jeffreys, *Theory of Probability*, 3rd ed. (Oxford University Press, New York, 1961).
- [54] <http://desi.lbl.gov/>.
- [55] N. Benitez *et al.* (J-PAS Collaboration), [arXiv:1403.5237](#).